LA-UR-21-30434

Title: TRUST Contact Thermal Conductance (CTC) Report

Author(s): LeBrun, Thomas John
Brindley, Kyle Andrew

Intended for: Report

Issued: 2021-10-20

TRUST Contact Thermal Conductance (CTC) Report

Release FY21.0.4.dev147+ge512983.d20211019

Thomas J. LeBrun, Kyle A. Brindley

Oct 19, 2021

CONTENTS

The objective of the Delivery Environments (DE) Testbeds to Reduce Uncertainties in Simulations and Tests (TRUST) work package is to quantify and help increase confidence in specific areas of computational and experimental capabilities that are applicable to current and future delivery environments. More complete quantification of confidence in experimental and computational capabilities and the sufficient increase of confidence in those capabilities is critical to improving weapons engineering design, qualification, and assessment efforts that are critical to the current and future stockpile. Staff development will include cross-discipline training to provide engineers with experience in both numerical simulations and experimental methods. This work will use and provide feedback on analysis tools and experimental results databases for efficient and responsive engineering which are currently under development: engineering common model framework (ECMF), engineering quantification of margins and uncertainties (EQMU), and the test information management system (TIMS).

TRUST includes four testbeds and their associated engineering analysis baseline models (EABMs):

1. contact thermal conductivity (CTC)
2. nonlinear dynamics (ND)
3. sensors in environments for accelerometers (SEA)
4. sensors in environments for fiber optic displacement gages (SEFOD)

CHAPTER

ONE

INTRODUCTION

"(U) Single Feature Testbeds to Reduce Uncertainty in Simulations and Tests" [1] provided an overview for the need of experiments, with accompanying models and simulations, specifically designed to reduce uncertainties and build confidence in complex testing and analysis applications. The Contact Thermal Conductance (CTC) testbed is a joint effort between W-13 (formerly E-13) and MST-8. The objective of this study was to design a testbed, with accompanying finite element models, to quantify, reduce, and propagate measurement uncertainties in contact thermal conductance measurements between two mating components in WR-like thermal environments. The knowledge gained through this simplified experiment would educate more complex assessments and interaction conditions with WR-like materials and geometries.

CHAPTER

TWO

EXPERIMENTS

2.1 Experimental Summary

"Experimental Procedure and Results for Contact Thermal Conductance Measurements performed during FY 2021" [2] provides the detailed experimental procedure conducted in MST-8. The testing fixture changed from the previous efforts presented in [3] while the procedure remained the same. The testbed (Figure 2.1) is a derivation of the ASTM E1225-13 [4] standard and included two metallic right cylinder specimens in contact with each other inside of a MTS-359 servo-hydraulic load frame that produce varying contact pressures. The load frame had hot and cold fixtures that produced a thermal gradient across the specimens. Data is collected using the load cell and LVDT inside of the MTS-359 machine and numerous thermocouples (TCs) at specified locations across the system.

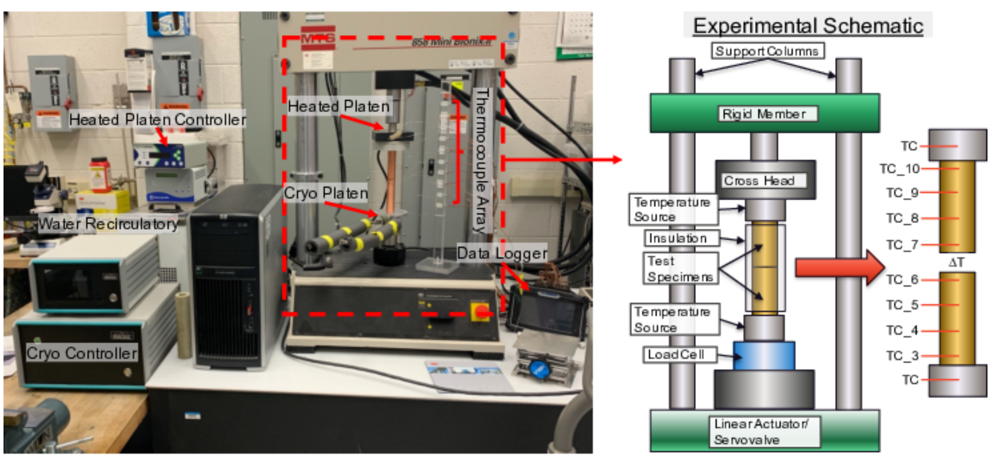

Fig. 2.1: CTC Experimental Setup (left) and Schematic (right)

Figure 2.1 (modification of [2]) depicts a mock experimental setup using copper samples to assess and learn how to operate the system and the experimental schematic showing the TC locations. Not shown is the insulation package used to reduce heat loss to the environment. The actual test specimens are cold drawn SS-304/304L and AMS 4117 Al-6061-T6. The samples feature either a smooth (0.8 micron) or rough (1.6 micron) surface roughness typical of WR-like components and used to study the effects on the interface conductivity. Conductivity measurements of the materials were collected to further reduce the uncertainty of the system [2].

The fiscal year 2021 (FY21) experiments were conducted on all sample combinations for the 1.6 micron samples. Each loading condition included at least two repeat tests (for a total of 3 tests). Only the SS-304 to SS-304 were fully vetted for FY21. Fully vetted includes post processing and upload of the data into the Test Information Management System (TIMS [5]). Figure 2.2 shows the temperature profile across TC-7 and TC-6 (reference Figure 2.1) for all SS-304 to SS-304 experiments.

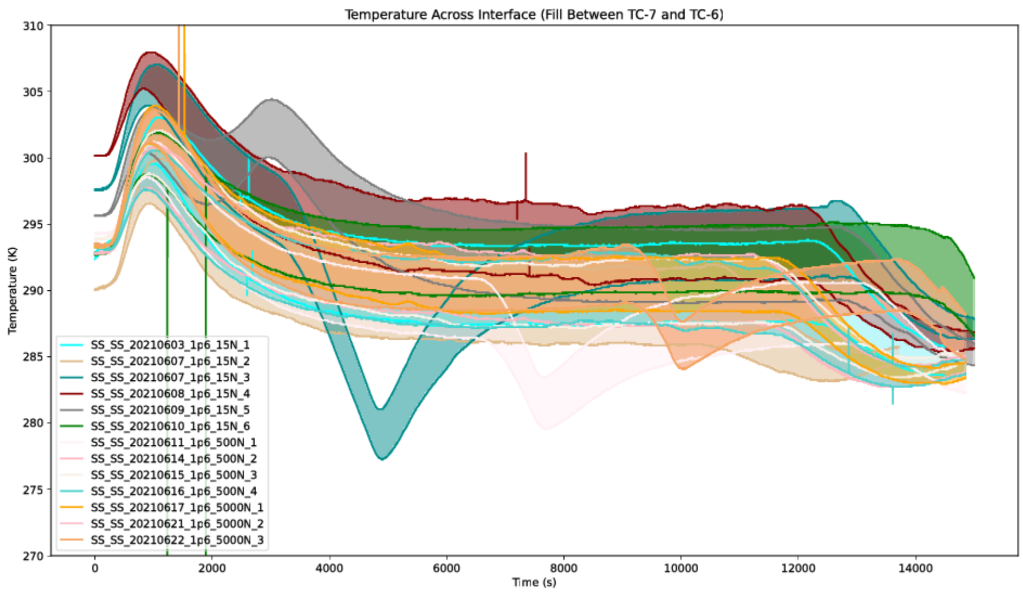

Fig. 2.2: Experimental Interface Temperature Gradient for TC-7 to TC-6

For clarity, Figure 2.2 only shows the output for TC-7 and TC-6. The solid lines are the actual TC output while the semi-transparent sections help map TC-7 to TC-6 for a given experiment. Note, the temperature drops observed in 15N_3, 500N_1, and 5000N_2 experiments were caused by facility issues that prevented the heated platen from operating properly.

CHAPTER

THREE

MODEL

The CTC model finite element model is designed to accurately represent and simulate the MST-8 CTC TRUST testbed. The Abaqus 2019 model is a transient coupled temperature-displacement 2D axi-symmetric model with the system aligned along the 2-axis as the axis of symmetry as shown in Figure 3.1. The model includes: two samples with pressure dependent contact at sample interface, surface film boundary condition to the environment, partitions at each TC location for comparison to test data, concentrated force distributed to top sample top surface in negative 2-direction via a reference point and rigid coupling, and temperature variation defined on top and bottom samples at TC locations near the experimental platens that would induce a thermal gradient across the system.

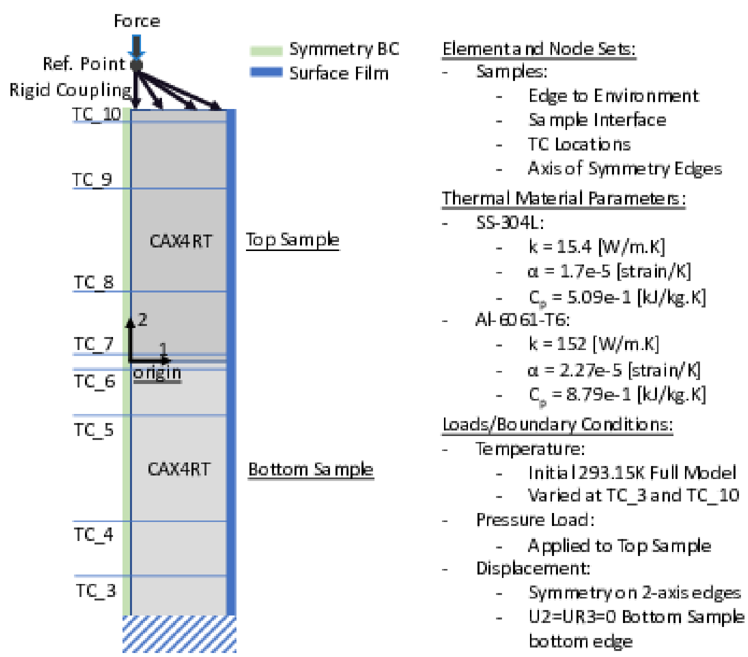

Fig. 3.1: TRUST Contact Thermal Conductance Model Defintion

The testbed contains various measurements, such as sample dimension, that contain measurement uncertainties. These measurements motivated a parametric build approach that allow studies to be conducted on these measurements. The model is built using Cubit 15.5 [6], where Cubit variables [7] can be leveraged to easily change the various parameters. The geometry, partition, and mesh parameters are contained in a single include file via the ECMF capabilities. The capabilities of the ECMF are documented at [8].

3.1 Geometry

The CTC model, in Figure 3.1, includes both samples with nominal dimensions 100mm x 12.7mm. The geometry stack up is: top sample, bottom sample.

3.2 Boundary Conditions

Y-symmetry (U1=UR2=UR3=0) is applied to all parts on their 2 axis edge as depicted as the green line on the left edge of the samples in Figure 3.1. Note a 2D-axisymmetric model only has 3 degrees of freedom (U1, U2, U3) so the y-symmetry boundary condition is used for simplicity in the input file. The bottom edge of the bottom sample is fixed with an ENCASTRE boundary condition to represent the rigid test fixture. An initial temperature boundary condition of 293.15K is applied to all parts. The subsequent steps vary the temperature in time of the TC near the ends of the samples in accordance to the experimental output. It is important to note that an additional static step was required prior to the transient thermal loading step for convergence reasons. The static step was an initialization step to the initial temperatures of the experiment as direct solving from the 293.15K to the initial temperature conditions caused numerical issues that would crash the simulation.

3.3 Loading Conditions

The experiment includes an applied load to control the contact pressure (shown in Figure 3.1 as a force arrow on the reference point coupled to the top sample). A concentrated force is applied to a reference point that is rigidly attached to the top surface of the top sample in the negative 2-direction with the magnitude varied in time according to the experimental output while a surface film load is applied to the free edge of the parts. The rigid coupling to the top surface results in a uniform load on the system.

3.4 Element Type

All parts in the CTC model are assigned continuum axisymmetric coupled temperature and displacement with reduced integration (CAX4RT) element type. More about axisymmetric continuum elements can be found in the Abaqus element documentation [9].

3.5 Interactions and Models

The CTC model includes two interactions: 1. sample-to-sample interaction, 2. system-to-environment modeled as a surface film. The sample to sample interface is modeled with penalty friction, a tangential coefficient of 0.4, hard overclosure, and gap conductance as a function of contact pressure. The nominal gap conductance are taken from system level models that were used in previous assessments and are listed in Table 3.1. The gap conductance values can be modified as experimental data is obtained.

Table 3.1: Initial Gap Conductance Values

Conductance [N/mm.K]	Pressure [MPa]
0	0
5000	1
10000	10

The experiment includes an insulation package to reduce heat flux to the environment (depicted as the blue line on right edge of the samples in Figure 3.1). The insulation package is modeled using a surface film where the film coefficient could be set to values similar to the experimental setup. Information on the Abaqus surface film modeling can be found as [10].

CHAPTER

FOUR

RESULTS

4.1 Sensitivity Study

The results from [11] lead to more accurate quantification of the input uncertainty. However, the updates to the input distributions required an understanding of their effect on the system. The nominal TRUST-CTC model was updated with a new loading scheme, new distributions on the parameters, and was analyzed based on SS-304l to SS-304l system. The updated input distributions are given in Table 4.1.

Table 4.1: Input Parameter Distributions

Parameter	Distribution Type	Distribution Parameters	Description
Surface Film	Uniform	Lower = 0.5313, Upper = 1.018	Convection coefficient representing the insulation package with the lower bound including low ambient air and upper including forced air.
Gap Conductance	Uniform	Lower = 0.8, Upper = 1.2	Gap conductance multiplied by distribution. The distribution for the nominal build is a wide uniform range. The actual experimental distribution is Normal with mean = 1 and std = ~0.02-0.15.
Material Conductivity	Normal	Mean = 1, STD = 0.1	Temperature dependant conductivity of material multipled by the distribution.
LC/BC* Magnitude	Uniform	LC: Lower = 0.955, Upper = 1.05, BC: Lower = 0.9925, Upper = 1.0075	Magnitude of the loading or boundary condition (respectively) multipled by manufacture error range.

*LC are loading conditions and BC are boundary conditions.

The temperature difference across the sample-to-sample to interface is used as the output metric to assess the influence of the model inputs. To stay consitent with the experiment, the difference between nodal locations at TC-7 and TC-6 is used. The model was simulated ten times, a reduced order model (ROM) was created and assessed using Studentize SVD decomposition and Kringing Vector mapping [12]. The subsequent ROM is evaluated for modal contribution and screened for parameter effect in each mode. It was found that the first mode contained 99.0212% of the information to recreate the model response. The parameter effect is presented in Figures 4.1 and 4.2 where the first mode is Mode 0.

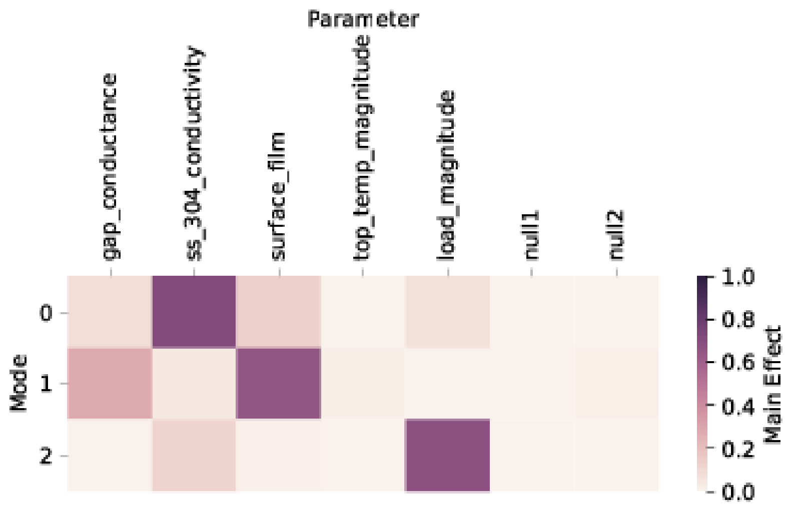

Fig. 4.1: Parameter Main Effect on Model Response

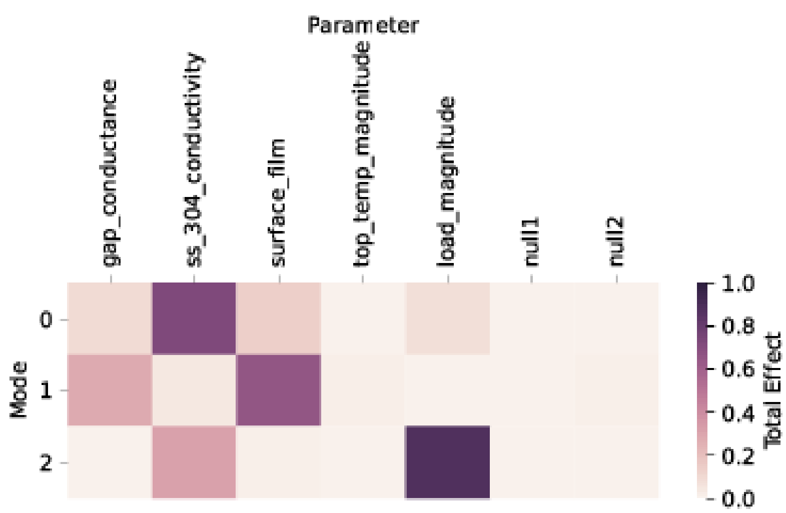

Fig. 4.2: Parameter Total Effect on Model Response

Note, that the main effect represents the effect of parameter if it were the only parameter in the model while total effect considers interactions between the parameters.

4.2 Experiment Comparison

The experiments presented are the well vetted experiments from Fiscal Year 2021, as described in [2]. These include SS-304l to SS-304l, with a rough surface finish (1.6 micron), and target contact pressures of 0 MPa, 1 MPa, and 10 MPa. There were a minimum of three experiments for each loading condition. The experimental results were pre-processed to produce loading amplitudes, temperature boundary conditions for TC-3 and TC-10, and gap conductance values that were integrated into the model. Further analysis of material conductivity experiments were also incorporated into the model.

The material conductivity is measured using the Hot Disk method. There were a total of ten measurements at three temperatures (~203, 293, 473K) to produce a temperature-dependent conductivity definition. A linear fit was calibrated to the data using a Bayesian calibration routine in Python. The results (shown in Figure 4.3) were then used in the model and in other calibration routines.

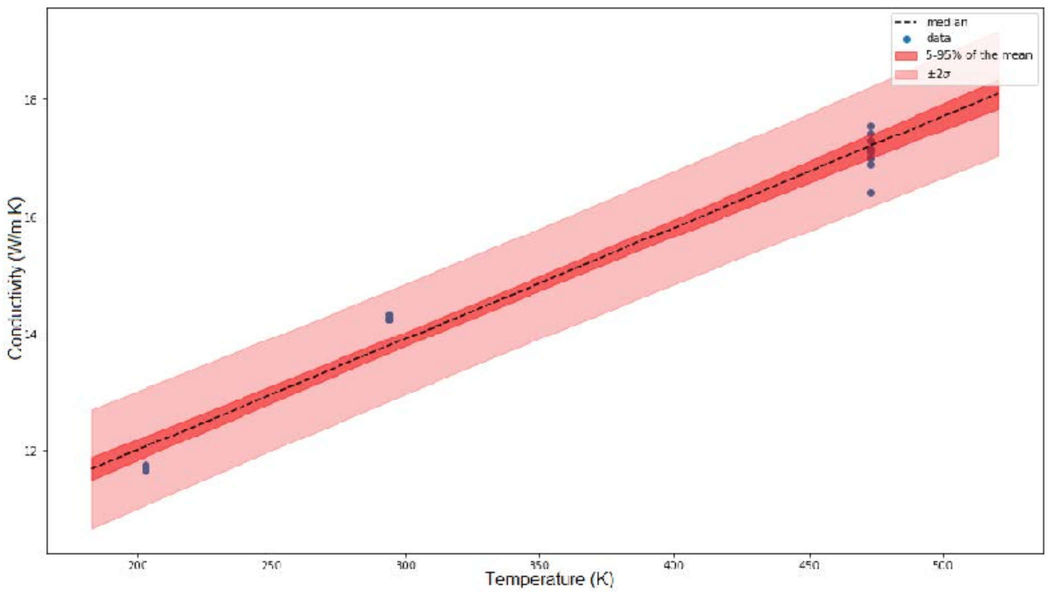

Fig. 4.3: Calibrated Linear Fit to SS-304l Conductivity Data with Uncertainty Bounds

Figure 4.3 shows the linear fit to the temperature dependent conductivity data. Included is the uncertainty bounds for the 5% and 95% quantile and two standard deviations.

All experimental uncertainty was considered when calculating the interface conductance value for the experiments including: +/- 2.2K error in the thermocouples, material conductivity and measurement error in the micrometers and toolmaker microscope (used to located the thermocouples on the samples) [2]. The interface conductivity is calculated using a Fourier Series of resistors where the values of the resistors is calibrated to the thermocouple measurements. All experiments are used in this calibration. Only the average of the steady-state points for the experiment were considered (Figure 4.4. The steady-state is determined by the points in time where the difference in the interface temperature does not change more than 0.25K.

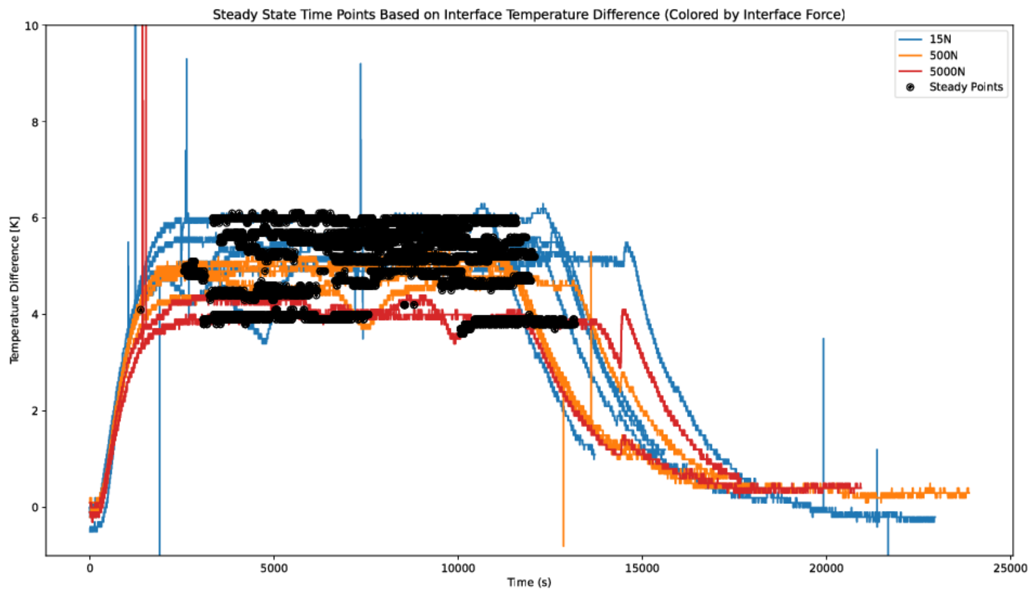

Fig. 4.4: Determined Steady-State Data Points for each Experiment (Colored by Interface Pressure)

Figure 4.4 shows the steady-state points (black points) calculated by a Python algorithm for each of the experiments. The colored lines represent the different interface pressure conditions. The assessment of these points produces the steady-state interface conductance value long with uncertainty values on each form of measurement that is used in the model. The steady-state points are also used inversly to downsample the time series data to create Abaqus amplitude boundary conditions for the transient portions of the experiment to be used in simulations. This pre-processing of the data reduces the simulation run time in favor of large parametric studies. The following figures compare the model response with the calibrated values to the experimental output. Note, only the last experiment for a loading condition is shown with all experimental comparisons presented in Appendix A.

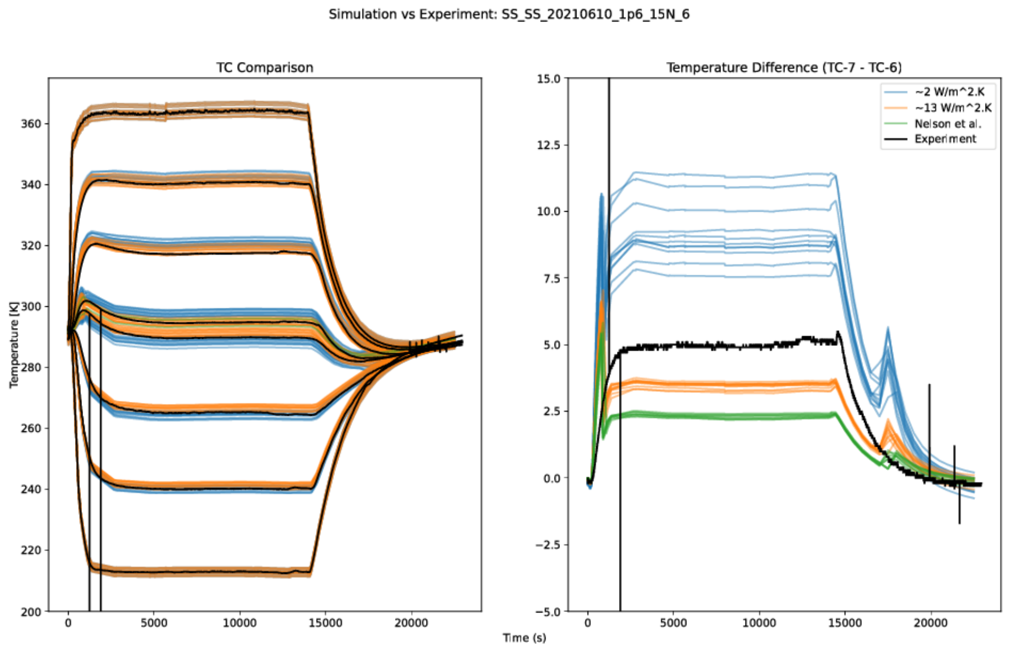

Fig. 4.5: 15N (0 MPa): Simulation and Experimental Results with Interface Temperature Difference

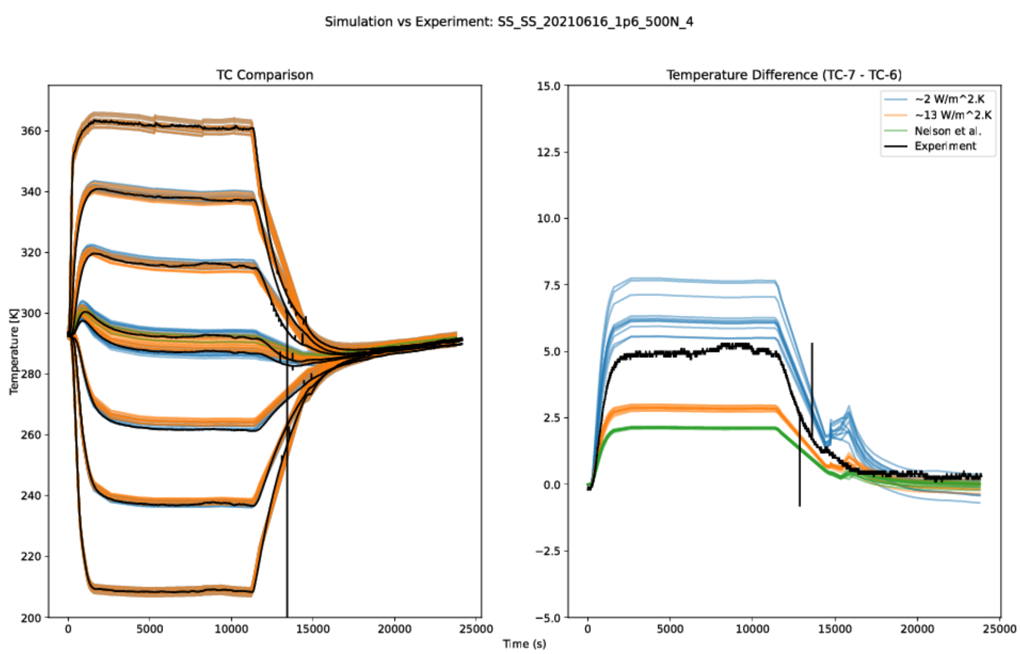

Fig. 4.6: 500N (1 MPa): Simulation and Experimental Results with Interface Temperature Difference

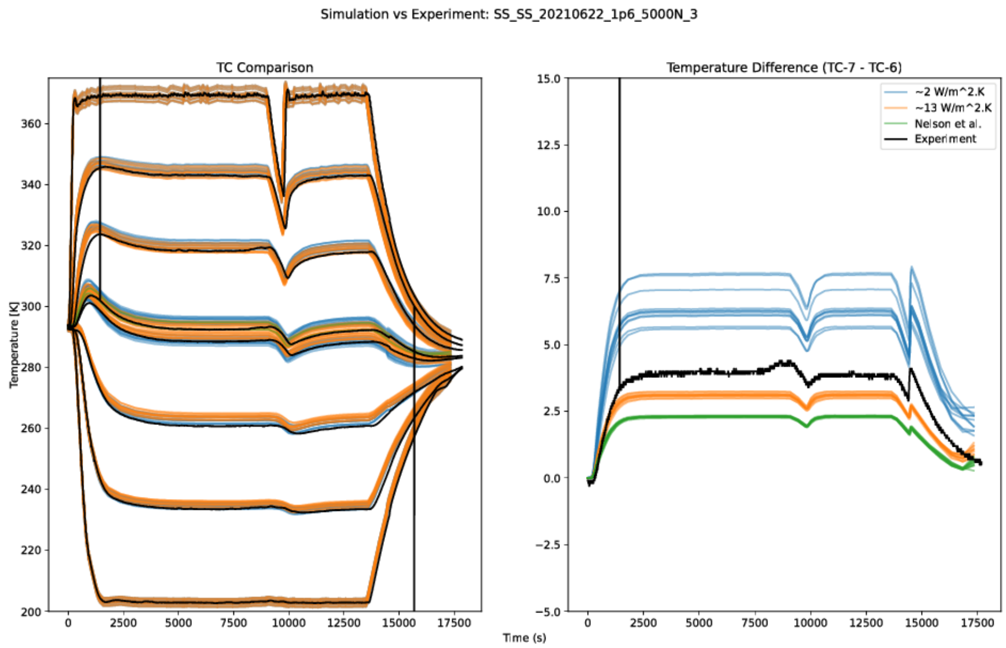

Fig. 4.7: 5000N (10 MPa): Simulation and Experimental Results with Calculated Interface Temperatures

Figure 4.5 through Figure 4.7 show the model response (blue, orange, and green curves) in relation to the experimental results (black curves) with the temperature difference across the interface. The legend shows the values of the interface conductance in relation to the colored output. The values for "Nelson et al." are found in [13] and range from ~3000-11200 W/m^2.K. The discrepancies between the model and the experiment are discussed in the *Discussion* section. The 2 W/m^2.K and 13 W/m^2.K were calibrated in the same model to test two different analysis methods found in literature [13]. The 2 W/m^2.K is calculated directly from the calibrated interface resistance as 1/RA where R is the resitance of the interface and A is the contact area of the interface. The 13 W/m^2.K was calculated using near interface values as a subset Fourier series using the calibrated values of material conductivity, and contact resistance [14].

CHAPTER

FIVE

DISCUSSION

5.1 Results Discussion

The results presented in the *Experiment Comparison* section shows that conductance values found in literature (presented in [13]) fail to produce the interface temperature drop in the FE simulations that was measured in the experiments. The values calculated from the experiments were significantly smaller (orders of magnitude) but represented the experiments more accurately. The temperature gradient across the system (measured at specified loactions thermocouple loactions) is a function of the conductivity of the material and the conductivity of the interface. The conductivity of the material was further measured in order to reduce the uncertainty in the calculation of interface conductivity and in the FE simulations. However, it must be noted that material conductivity measurements could be leading to the errors that are seen. Figure 5.1 shows similar experimental measurements with statistically validated material data from MMPDS-13 [15].

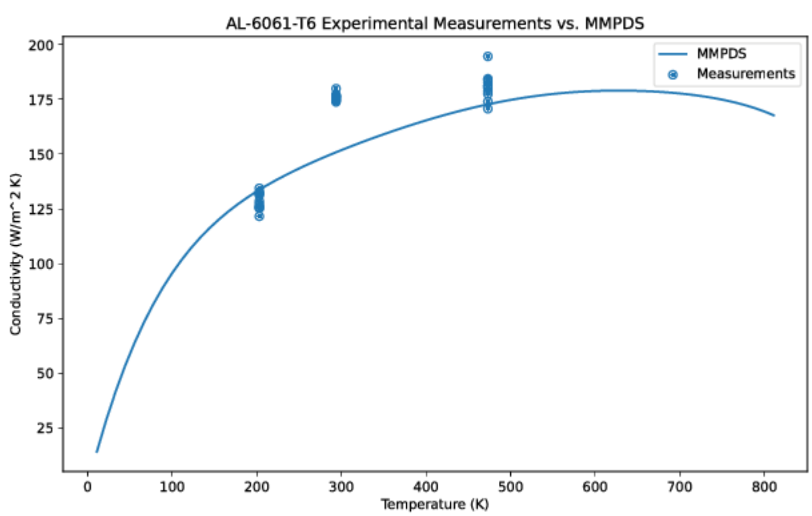

Fig. 5.1: AL-6061-T6 Thermal Conductivity Measurements with Attemped Fits Compared to MMPDS Data

Figure 5.1 shows the measured conductivity values and the statistically validated data for the pedigree of AL-6061-T6 that was purchased for this study. The measurements at 203K and 473K agree with the MMPDS-13 data with a large discrepency in the room temperature (293K) measurements. The data at 293K does not display a large variance but is 120% greater than the MMPDS-13 values, indicating that either the material is not consistent with it's specification or the experiement was not conducted properly. The later is under investigation as the experiemental measurement requires numerous inputs for the conductivity calculation :cite"*Valdez_CTC-FY20*. Similar statistically validated data does not exist for the SS-304L material. Both Figure 4.1 and 4.1 show that the material conductivity has a large effect on the model response for the quanty of interest (temperature difference across the interface) and although the measured values produced similar response to the experiment, they need further validation.

The results presented in the *Experiment Comparison* section also show that the interface conductance is between 2 and 13 W/m^2.K for these experiments. The ~2 W/m^2.K values (blue curves in Figures 4.5-4.7) produced a high predicted temperature difference, ~13 W/m^2.K (orange curves) predict a lower temperature difference, with the 3000-11200 W/m^2.K (Nelson et al. curves) predicting the lowest interface temperature difference.

The results provide insight into potential errors with the model inputs. The temperature across the system, including the interface, is a function of heat transfer through the system. The heat transfer is dictated by the various conductance coefficients including gap conductance and conductance of both materials. A more accurate representation of the conductance values is needed to validate the model to the experimental results. MST-8 was tasked with measuring the material conductance which is presented in the experiment report [2]. The measurements showed a potential source of error and will be reevaluated.The updated resulting output will be compared to previous analysis to assess the effects of the changes.

Lastly, the calculated values are significantly different from the values used in legacy models. The values, with their uncertainty, will be incorporated into legacy system models to investigate their effects on previous assessments. The knowledge learned from this exercise will present evidence that the calculated values are either in the correct range or if the experiment needs to be re-designed.

5.2 ECMF Discussion

The Engineering Common Model Framework (ECMF) [16] was used as the simulation manager for the various models in TRUST-CTC. At the time of reporting it was in version 0.5.6 with full release being indicated as version 1.x.x. Thus, it was still under development as a beta release with most of the intended functionality available. There are positives and negatives to the state of the ECMF used in this study as viewed by the author:

Positives

- Support of any distribution type found in the Scipy Python library
- Intuitive workflow
- Advanced feature support such as Python string templates
- Inclusion of Engineering Quantification of Margin and Uncertainty (EQMU)
- Multiple parameter techniques (Cartesian Product and Latin Hypercube sampling)

Negatives

- Documentation lacks instruction for more advanced feature such as Python string template
- EQMU is not directly integrated
- Workflow is susceptible to breaking as more advanced techniques are used
- The current framework fails to write anything of importance (workflow step information) to the output hdf5 file when using some ECMF workflow steps (i.e. Spawn)
- No restart capability which leads to rerunning analysis if a portion of the workflow fails
- New preference for Latin Hypercube sampling provides only basic operations and does not allow for tabular modification without external scripting

5.3 GRANTA Discussion

GRANTA is a commercial database that is used at LANL for material data storage (Material Information Management System [MIMS] [17]) and is being tested as a storage solution for experimental data (Test Information Management System [TIMS] [5]). GRANTA provides the basic framework and tools to create and use a custom database which has proven to be ideal when working with LANL type data. Both MIMS and TIMS were used to communicate and store the data collected as part of the TRUST-CTC testbed.

The material specific information (material conductivity) was stored in MIMS while all information pertaining to the experiments was uploaded into TIMS. The MIMS database is well established and can handle the types of data that was being uploaded; however, the TIMS database is in a beta phase and required further development to handle the various data types that were being uploaded. For example, it only included data types for sensors already converted into engineering units rather than raw voltage output (e.g. temperature for thermocouples). Attributes to handle raw voltage output from sensors had to be added to accommodate some of the raw data sensors that were used in the tests.

The raw data was modified through means of python scripting that would convert the raw voltage signal into engineering units, while shifting the data in time to align the various records, and scaling the time axis due to measured lag between the data acquisition systems. The processed data was then added to TIMS as a "derived" sensor. This process was clunky for the following reasons:

- Loading the data into python was non-trivial and the GRANTA python package can be difficult to learn.
- The GRANTA STK Python methods require specific search terms and cannot be generalized to suite all querying applications
- Navigation in GRANTA STK of the GRANTA records required opening multiple GRANTA tables that contain large amounts of data and is slow
- The data had to be manually uploaded back into TIMS
- Data was subject to duplication as the process is manual and prone to user error

The benefits to the TIMS database include:

- Inclusion of multiple types of data (i.e. experimental schematics to accompany time-series data)
- Ability to modify the types of data included in a record (adding new attributes for pertinent information)
- Familiarity to MIMS database makes navigation trivial
- Potential for confusion in the sensor convention that the database is based on

CHAPTER SIX

FUTURE WORK

The CTC workflow is designed to provide a validated model to accompany the experiments. This included: experimental measurements to provide model inputs, and model results provided guidelines for experimental measurements. The values measured and calculated support the response of the physical system but the values are significantly different than those found in literature. Exploration of the conductivity values found and their implementation into a finite element solver needs to be conducted so that future modeling efforts are capturing the correct response.

Further experiments were devised with modifications to the experimental procedure. The identified issues were: data acquisition system errors to collect the correct load and displacement measurements channels, further material testing to reduce uncertainty into material conductivity, relative error experimentation of the thermocouples. Further experimentation will provide insight into the response of the system and reduce uncertainties in the measurements that will be propagated through the pre-processing of the model inputs for continued iterations of the workflow.

Further analysis development will be devised to more accurately evaluate the experimental data prior to implementation into the finite element model. These changes include: updated sampling methods in Python, and alternate form of the contact conductivity calculation other than the Fourier Series.

Further exploration of the model will provide additional insight into the sensitivity of the model to various model inputs. The model will take advantage of the future development work in the W-13 EQMU tools. These results will further guide the experiments.

CHAPTER

SEVEN

CONCLUSIONS

The CTC testbed was designed to quantify thermal conductance across an interface as a function of surface roughness and contact pressure. A finite element model was created in the engineering common model frame work for comparision to the experimental configuration as well as validate interaction models to be used in more complex analysis.

Discrepancies were observed between the simulation output and experimental results. Exercising the model provided guidance for future testing in order to reduce uncertainties in the model. This guidance included refining the temperature profiles of the experiment, material characterization, and data acquisition syncing. The future results will update the model input where validation can be assessed. Further propagation of error in the experimental measurements needs to be explored in order to provide a validated model that accurately captures the experimental results.

The model input needs to be evaluated using reduced order modeling tools to provide additional guidance for experimental measurements. The results will also provide insight into other potential sources of error such as model form error where parameters like loading definition, boundary condition definition, and mesh could be contributing to discrepancies between the model results and experimental results.

CHAPTER

EIGHT

ACKNOWLEDGMENTS

The author would like to acknowledge the experimental efforts put forth by MST-8 that included:

- Saryu J. Fensin
- James A. Valdez
- Michael A. Torrez
- Carl M. Cady
- Talia M. Ben-Naim
- Nina A. Johnson

CHAPTER

NINE

APPENDIX A: EXPERIMENTAL COMPARISON

The following set of images are the experimental to simulation comparison for all of the experiments not presented in *Experiment Comparison*.

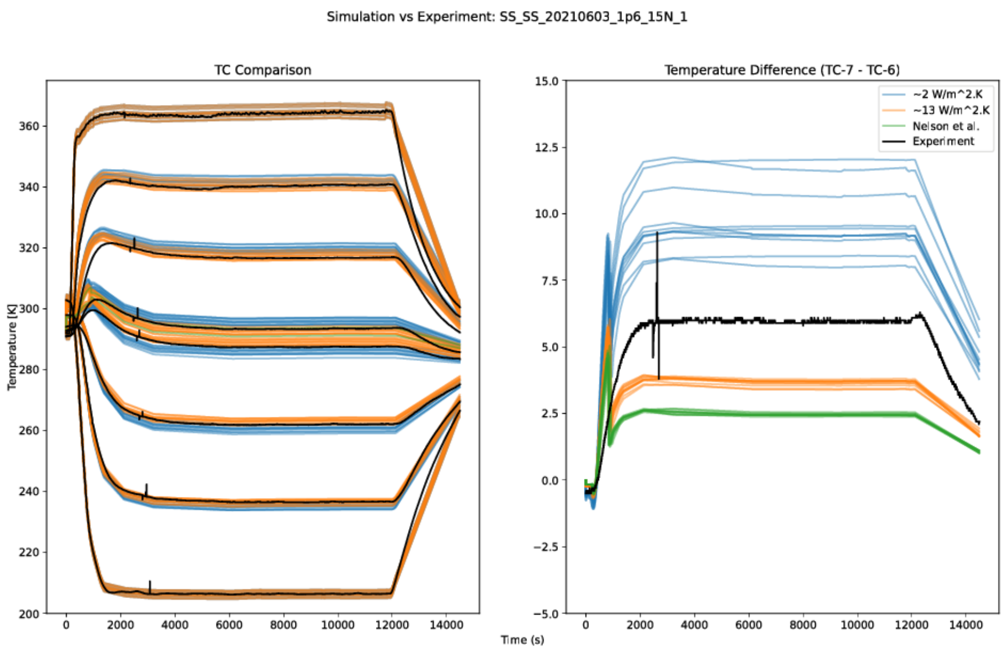

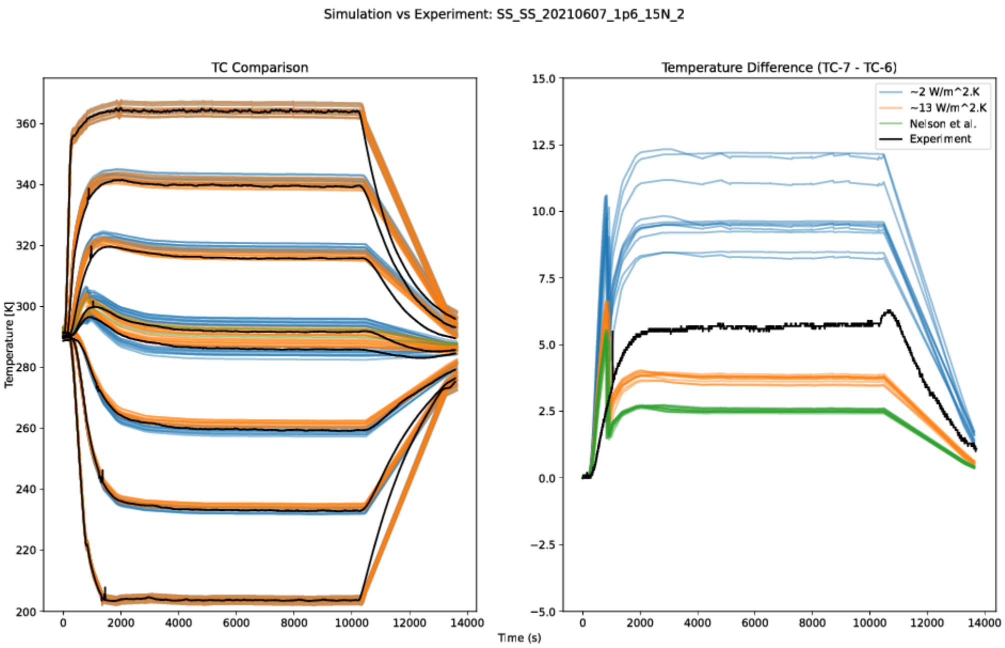
Simulation vs Experiment: SS_SS_20210607_1p6_15N_2
TC Comparison
Temperature [K]
Temperature Difference (TC-7 - TC-6)
~2 W/m^2.K
~13 W/m^2.K
Nelson et al.
Experiment
Time (s)

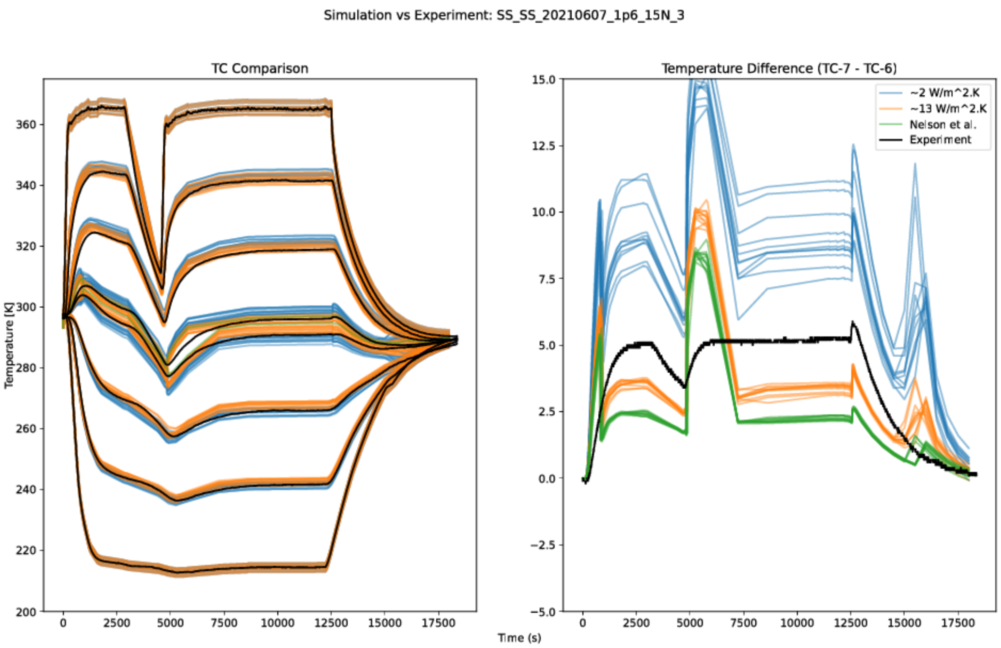
Simulation vs Experiment: SS_SS_20210607_1p6_15N_3
TC Comparison
Temperature [K]
Temperature Difference (TC-7 - TC-6)
~2 W/m^2.K
~13 W/m^2.K
Nelson et al.
Experiment
Time (s)

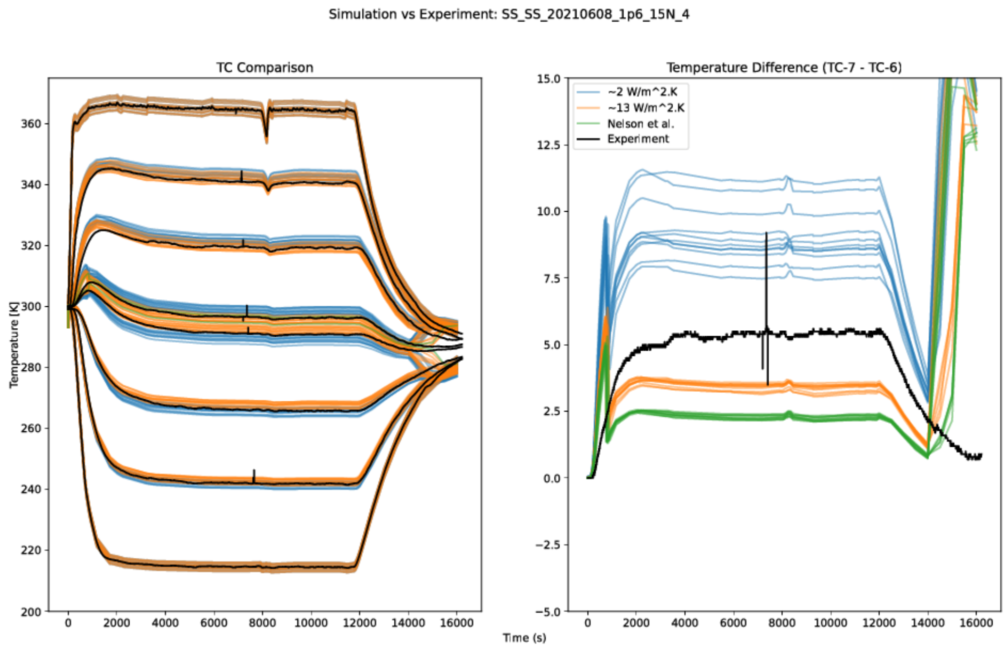
Simulation vs Experiment: SS_SS_20210608_1p6_15N_4
TC Comparison
Temperature [K]
Temperature Difference (TC-7 - TC-6)
~2 W/m^2.K
~13 W/m^2.K
Nelson et al.
Experiment
Time (s)

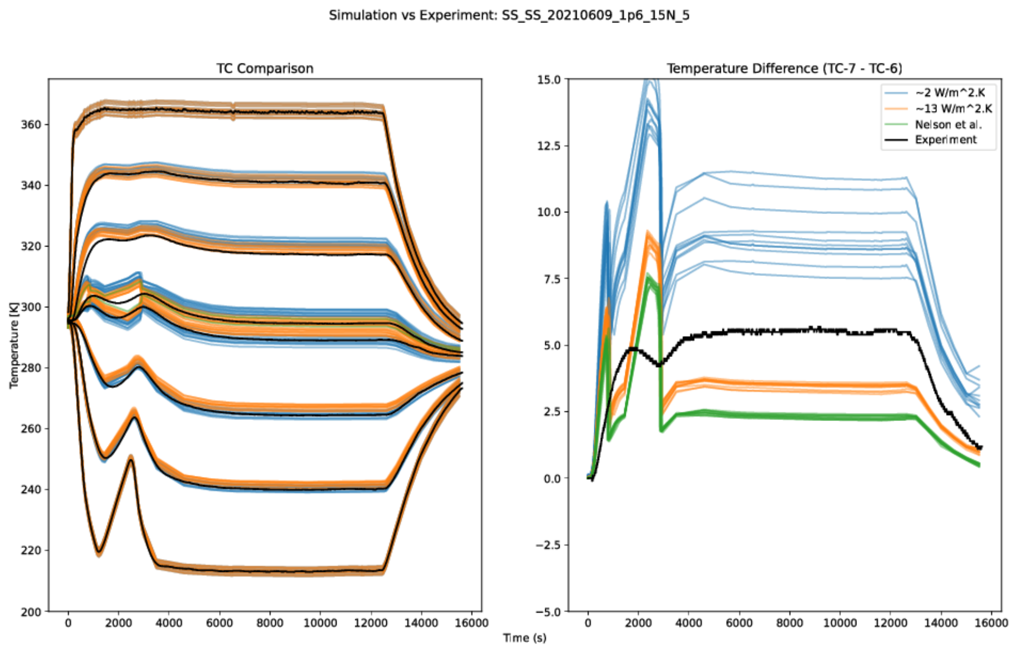
Simulation vs Experiment: SS_SS_20210609_1p6_15N_5
TC Comparison
Temperature [K]
Temperature Difference (TC-7 - TC-6)
~2 W/m^2.K
~13 W/m^2.K
Nelson et al.
Experiment
Time (s)

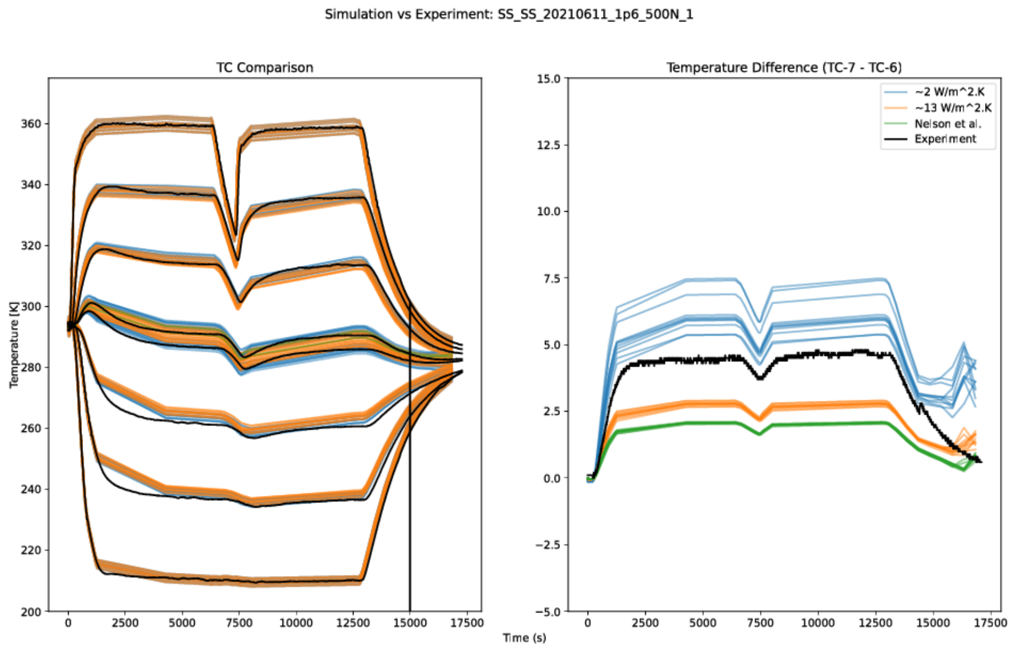
Simulation vs Experiment: SS_SS_20210611_1p6_500N_1
TC Comparison
Temperature [K]
Temperature Difference (TC-7 - TC-6)
~2 W/m^2.K
~13 W/m^2.K
Nelson et al.
Experiment
Time (s)

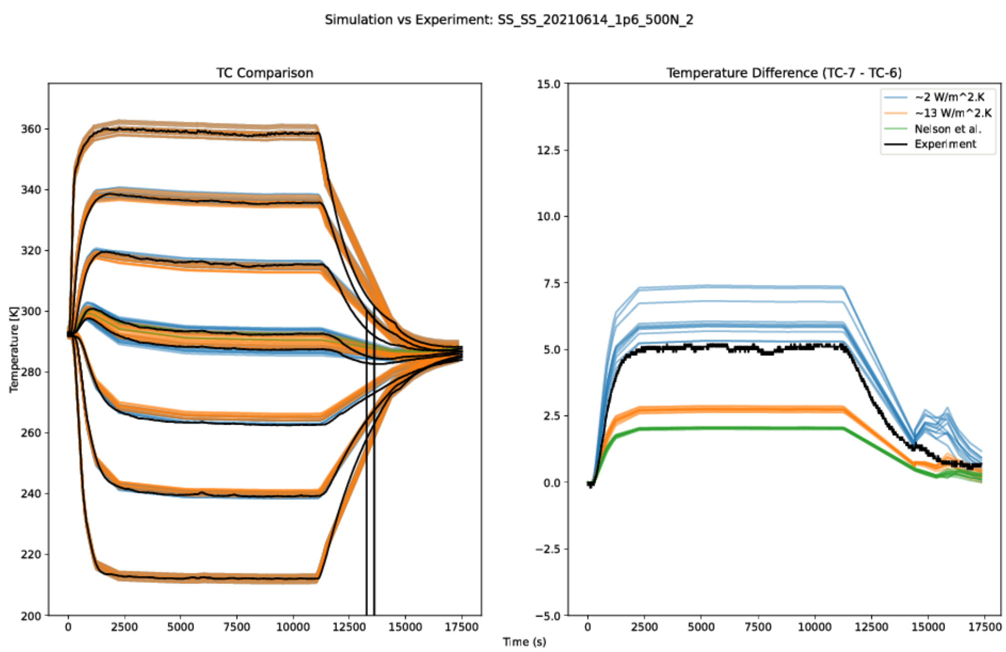
Simulation vs Experiment: SS_SS_20210614_1p6_500N_2
TC Comparison
Temperature [K]
Temperature Difference (TC-7 - TC-6)
~2 W/m^2.K
~13 W/m^2.K
Nelson et al.
Experiment
Time (s)

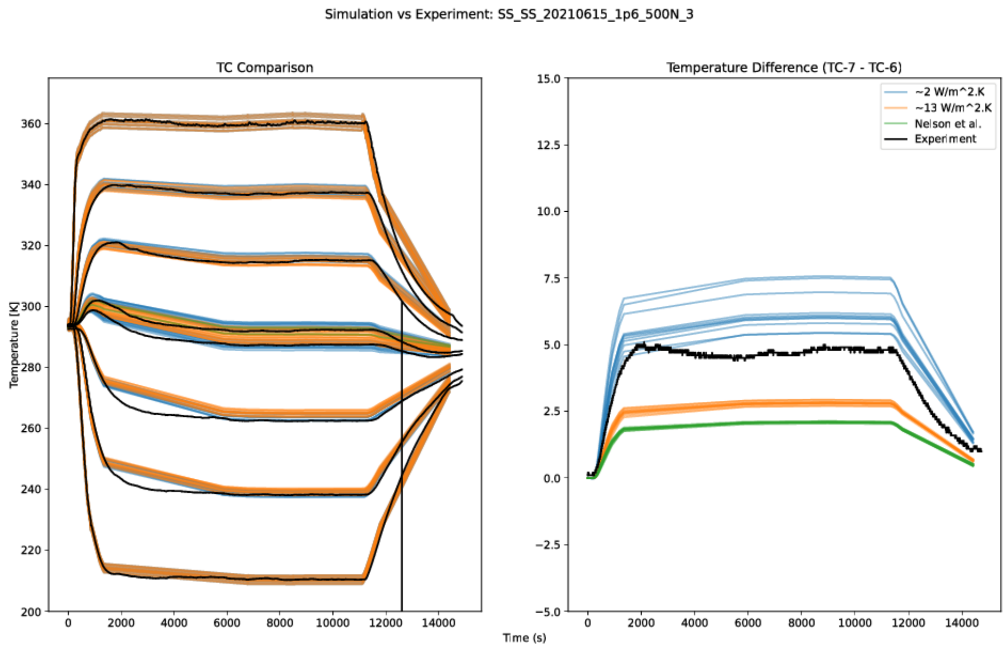
Simulation vs Experiment: SS_SS_20210615_1p6_500N_3
TC Comparison
Temperature [K]
Temperature Difference (TC-7 - TC-6)
~2 W/m^2.K
~13 W/m^2.K
Nelson et al.
Experiment
Time (s)

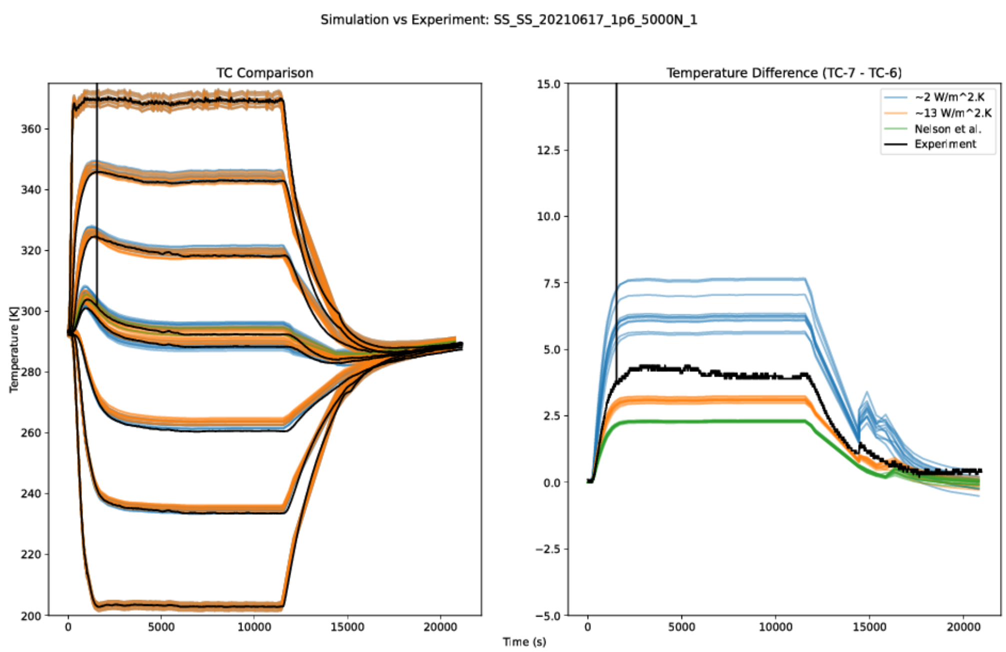
Simulation vs Experiment: SS_SS_20210617_1p6_5000N_1
TC Comparison
Temperature [K]
Temperature Difference (TC-7 - TC-6)
~2 W/m^2.K
~13 W/m^2.K
Nelson et al.
Experiment
Time (s)

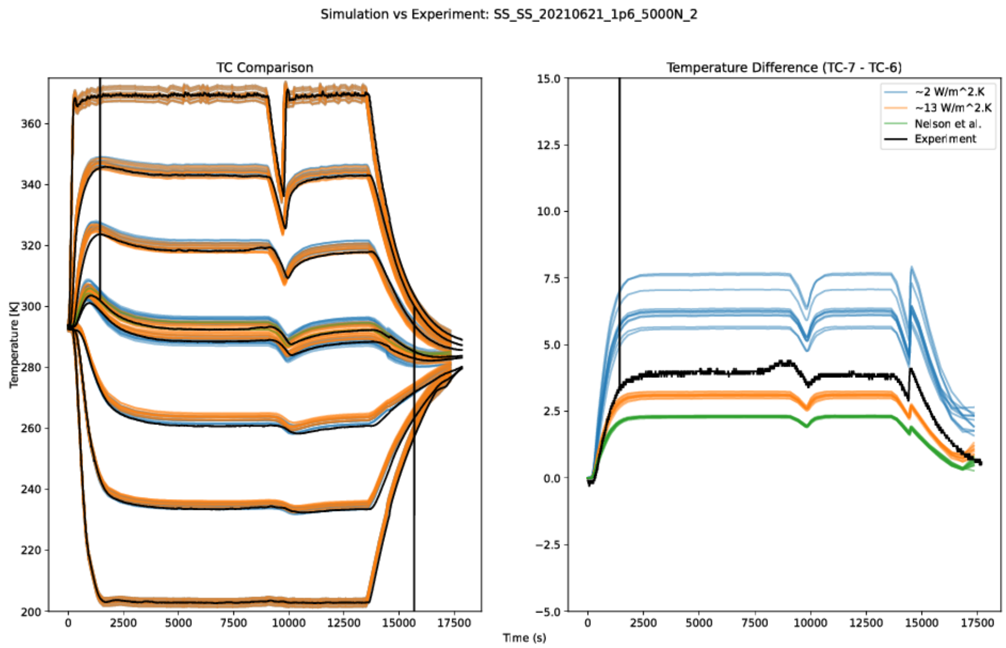
Simulation vs Experiment: SS_SS_20210621_1p6_5000N_2
TC Comparison
Temperature [K]
Temperature Difference (TC-7 - TC-6)
~2 W/m^2.K
~13 W/m^2.K
Nelson et al.
Experiment
Time (s)

BIBLIOGRAPHY

[1] Kyle A. Brindley and Antranik A. Siranosian. Single feature testbeds to reduce uncertainties in simulations and tests. Technical Report LA-UR-19-29860, Los Alamos National Laboratory, Los Alamos, New Mexico, USA, 2019.

[2] James Valdez, Carl Cady, Mike Torrez, Talia-Ben Naim, Veronica Anghel, Phil Schembri, and Saryu Fensin. Experimental procedure and results for contact thermal conductance measurements performed during fy 2021. Technical Report LA-UR-21-XXXXX, Los Alamos National Laboratory, Los Alamos, New Mexico, USA, 2021.

[3] James Valdez, Carl Cady, Mike Torrez, and Saryu Fensin. Experimental measurement procedure for performing thermal conductivity measurements in support of e-13 trust efforts. Technical Report LA-UR-20-27685, Los Alamos National Laboratory, Los Alamos, New Mexico, USA, 2020.

[4] ASTM Committee E37. Standard test method for thermal conductivity of solids using the guarded-comparative-longitudinal heat flow technique. Technical Report ASTM E1225-13, ASTM International, West Conshohocken, Pennsylvania, USA, 2013.

[5] Los Alamos National Laboratory. Test information management system (TIMS). 2020. URL: http://miweb/mi/index.aspx (visited on 2020-09-04).

[6] Sandia National Laboratories. Cubit 15.5. 2019. Albuquerque, New Mexico, USA.

[7] Sandia National Laboratories. Cubit 15.5: appendix: aprepro. 2019. Albuquerque, New Mexico, USA.

[8] Los Alamos National Laboratory. Engineering common model framework (ECMF). 2021. URL: https://aea.re-pages.lanl.gov/python-projects/ecmf/master/ (visited on 2021-09-21).

[9] Dassault Systemés Simulia Corporation. *SIMULIA User Assistance 2019*. Dassault Systemes, Providence, RI, USA, 2019. Abaqus: Elements: Axisymmetric Solid Element Library.

[10] Dassault Systemés Simulia Corporation. *SIMULIA User Assistance 2019*. Dassault Systemes, Providence, RI, USA, 2019. Abaqus: Loads: Thermal Loads.

[11] Thomas J. LeBrun. TRUST-EABM contact thermal conductance (CTC) report. Technical Report LA-UR-20-27413, Los Alamos National Laboratory, Los Alamos, New Mexico, USA, 2020.

[12] Los Alamos National Laboratory. Engineering quantification of margins and uncertainty (EQMU). 2021. URL: https://ddw-bitbucket.lanl.gov/projects/TOOL/repos/eqmu/browse (visited on 2021-09-23).

[13] Andrew Thomas Nelson. Measurement of contact conductance of 304L stainless steel and 6061-T6 aluminum interfaces through multilayer laser flash analysis. Technical Report LA-UR-15-29092, Los Alamos National Laboratory, Los Alamos, New Mexico, USA, 2015.

[14] Chakravarti V. Madhusudana. *Thermal Contact Conductance*. Springer, 2nd edition, 2014. ISBN 978-3-319-01275-9. DOI 10.1007/978-3-319-01276-6. doi:10.1007/978-3-319-01276-6.

[15] MMPDS-13 Database. 6061, t6, extruded rod, bar, shapes, thickness: 1.001 to 6.501 in, area: up to 32.001 sq in, ams 4150, a basis. Record History Guid:1025020a-a801-2301-0032-310650000100, Record Version Guid:1025020a-a801-2301-0032-310650000102.

[16] Los Alamos National Laboratory. Engineering common model framework (ECMF). 2021. URL: https://aea.re-pages.lanl.gov/python-projects/ecmf/dev/ (visited on 2021-09-21).

[17] Los Alamos National Laboratory. Material database. 2020. URL: http://grantami.lanl.gov/mi/index.aspx (visited on 2020-06-30).